COMPARISON OF STRONG MOTION AND WEAK MOTION RECORDINGS OF THE LOMA PRIETA SEQUENCE

O. Bonamassa, H. Houston, & J.E. Vidale

Earth Sciences Board
University of California
Santa Cruz, CA 95064

ABSTRACT

The Loma Prieta earthquake sequence has provided the opportunity to compare ground motion recorded both during an magnitude 7 mainshock and numerous magnitude 2.5 to 4.5 aftershocks at 14 sites. We find two results, (1) weak motion recordings of aftershocks have predictive power to indicate the directionality of the shaking in the mainshock, and (2) non-linearity during mainshock strong motions is suggested at the sites that suffered the largest accelerations in the mainshock.

INTRODUCTION

The Loma Prieta earthquake of 18 October 1989 was the largest to strike the San Francisco Bay area since 1906. It caused considerable damage and loss of life. On the positive side, this earthquake was captured by more than a hundred strong motion seismometers, producing an unprecedented opportunity to investigate details of the earthquake and earthquake hazards in general.

The earthquake resulted in thousands of aftershocks in the following months. Fourteen strong motion recording sites (shown in Figure 1) were provided with weak motion seismometers for various time intervals (Mueller and Glassmoyer, 1990). The combination of weak and strong motions allows us to test whether site characteristics estimated from the weak motions persist during damaging strong motions.

The motion that an earthquake causes at the surface of the Earth is a combination of the details of the faulting at depth and the complications due to propagation through structures within the Earth of the seismic energy released by the faulting. Various ways of measuring the seismic source and propagational complications have been described. There exists considerable literature that documents the usefulness of the concept of a *site response*, where a particular site has a fixed set of frequencies which are amplified at that site no matter how the how the ground motion is induced (Joyner et al., 1976, Rogers et al., 1984, Borcherdt, 1970, Joyner et al., 1981). Seismic wave interaction with large-scale structures such as major sedimentary basins can be described deterministically; these structures have been shown to distort seismic waves in a fairly predictable way (Vidale and Helmberger, 1988, Kawase and Aki, 1989, Kagami et al., 1986). Bridging the gap between well-understood large structures and small structures (for which only the amplitude versus frequency behavior has been studied) is the goal of considerable recent research.

We have suggested that the direction of shaking is sometimes a feature of the recording site rather than the earthquake (Vidale et al., 1991, Bonamassa et al., 1991, Bonamassa and Vidale, 1991, Vidale and Bonamassa, 1992). These and other observations of horizontal ground motion above one Hz frequency (Dietel et al., 1989, Abrahamson et al., 1989) show very small lateral correlation distances, less than 10's of meters for frequencies above a few Hz. Also, comparisons of seismograms written by surface and borehole instruments have shown that propagation through the shallowest 10's of meters of the Earth can severely distort seismic pulses (Haukkson et al., 1987, Malin et al., 1988, Aster and Shearer, 1991).

This report concentrates on quantifying empirically the distortion to the direction of strongest shaking and non-linearity caused by shallow earth structures.

DIRECTIONAL RESONANCES

For this presentation, we chose two stations that recorded many aftershocks with low noise. Our selection of the best-recorded aftershocks for each event, which are distributed over a wide area, as well as the station locations, are shown in Figure 2. 22 aftershocks were selected for station 378/AP7 and 25 were selected for station 006/GA2. 2 to 6 sec of the S wave, containing the largest accelerations, were windowed from the two horizontal components of each recording for the polarization analysis. The covariance matrix and its eigenvalues and eigenvectors were computed for each window. The direction of the eigenvector associated with the largest eigenvalue is the direction of the strongest shaking, and the ratio of the larger to the smaller eigenvalue is a measure of the signal linearity (Vidale, 1986).

Time domain information has been suppressed in this presentation, so it remains possible that the initial S-wave arrivals exhibit the polarization direction expected from the focal mechanism even at high frequencies, as has been observed by Bonamassa and Vidale (1991) and has also been observed for P waves by Menke and Lerner-Lam (1991).

Figure 3 shows the particle motion data for the two stations. The directions of shaking are evaluated in the frequency ranges from 0 to 1, 1 to 2, ... , and 9 to 10 Hz for each of the aftershocks and plotted as open circles. Though the pattern is more clear in the summary figures below, the tendency for some frequencies to vibrate in fixed directions at station 378/AP7 is apparent in Figure 3a. The highest frequency passband clusters strongly about NW-SE. There is also a concentration of points near E-W for the 1.5 Hz band. These clusters reveal directional resonances, where the site is most susceptible to vibrate in a fixed direction a some frequencies. We attribute this effect to local geology rather than a source effect since our previous works (Bonamassa and Vidale, 1991, and Vidale and Bonamassa, 1992 and others) show that there is generally little correlation between the particle motion predicted from the earthquake focal mechanism and the motion observed at these frequencies, and these resonance directions change between nearby stations. Station 006/GA2, in contrast, shows less clustering of the directions of strongest shaking in Figure 3b.

The overall coherence of the directional resonances is shown in Figure 4, which shows the *difference* between each aftershock polarization direction and the mainshock polarization at the same frequency. The mainshock direction is indicated by filled triangles in Figure 3. There is a strong central peak for station 378/AP7 in Figure 4a. Therefore the directions of motion in the mainshock correlate well with the directions in the aftershocks. Figure 4b, in contrast, shows that for station 006/GA2, there is little correlation between the mainshock motion and the aftershock motion. This plot is a conservative measure, since correlations would be more visible if passbands with higher linearity or more clustering of aftershock polarization were given more weight in the search for patterns. Note, for example, that the four passbands where the mainshock is most poorly polarized (2.5, 4.5, 5.5, and 9.5 Hz) show the least agreement between mainshock and aftershock directions for station 006/GA2.

Map of Cosited Instruments

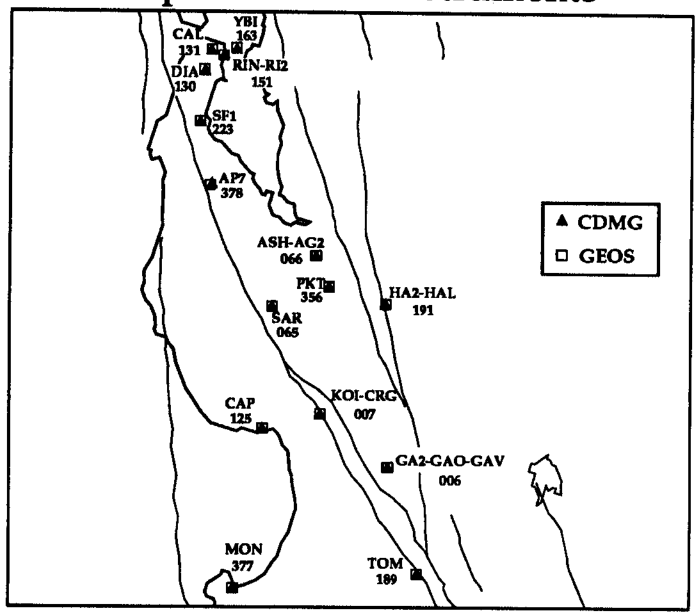

Figure 1. Map of stations recording both the mainshock and some of the aftershocks of the Loma Prieta sequence.

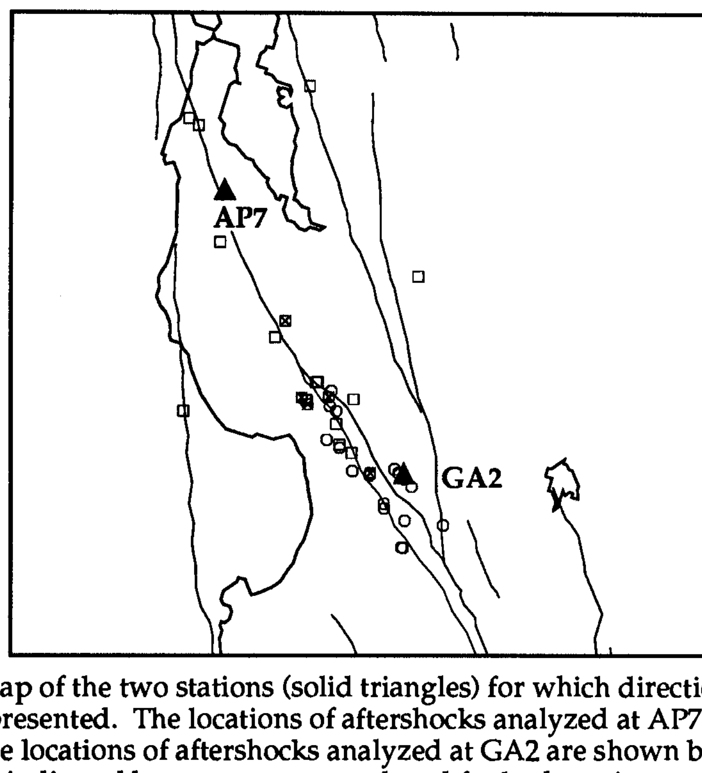

Figure 2. Map of the two stations (solid triangles) for which directional resonance analysis is presented. The locations of aftershocks analyzed at AP7 are shown by squares. The locations of aftershocks analyzed at GA2 are shown by circles. Aftershocks indicated by a cross were analyzed for both stations.

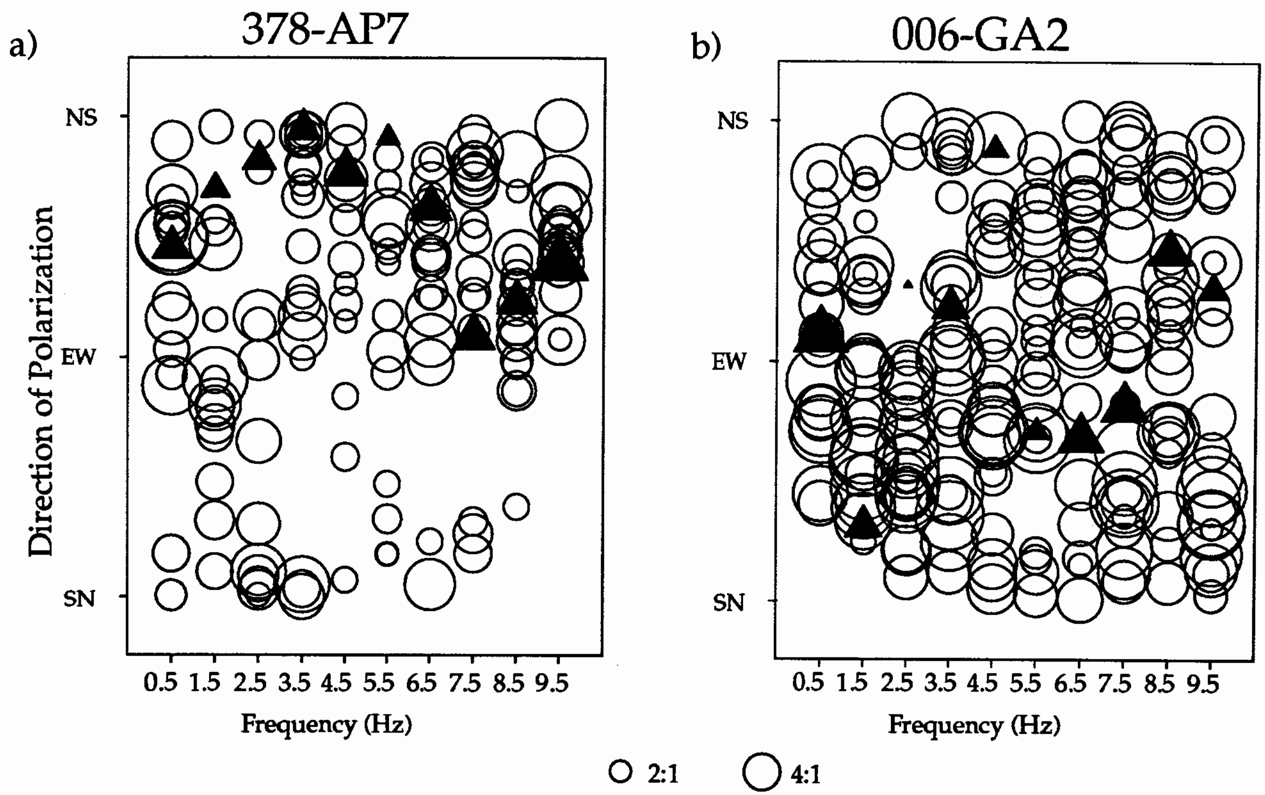

Figure 3. The preferred direction of motion plotted for each of the 10 frequency bands for each of the aftershocks. Larger symbols indicate more linear polarization. Solid triangles show the direction of polarization in the mainshock. Each frequency band is one Hz wide. a) Data from station 378/AP7. b) Data from station 006/GA2.

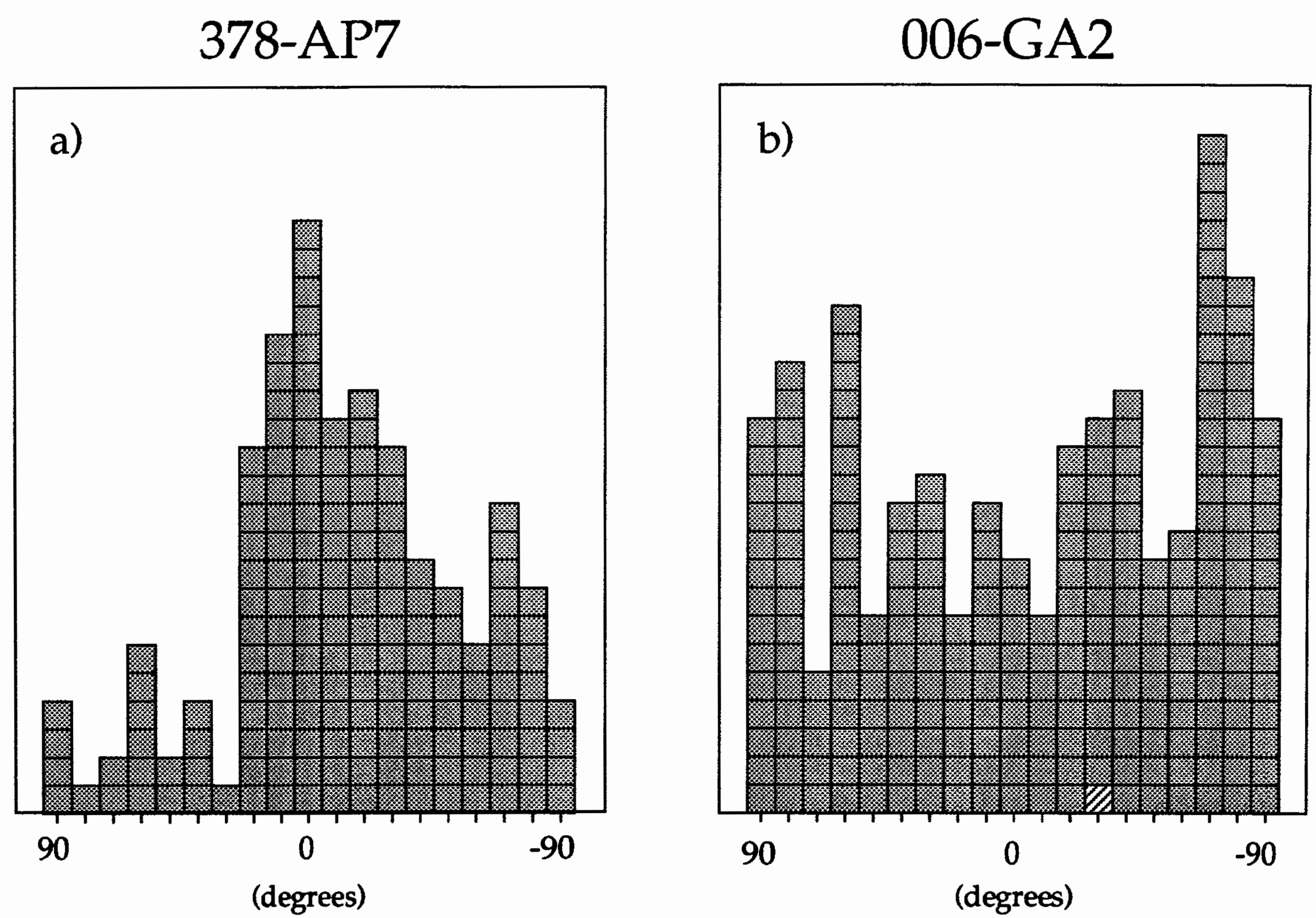

Figure 4. Histogram of azimuthal differences between the direction of strongest shaking in the mainshock and the direction of the strongest shaking in an aftershock for each aftershock and each frequency. a) Data from station 378/AP7. Note that the differences cluster around 0 to 20°. b) Data from station 006/GA2. The differences are not clustered.

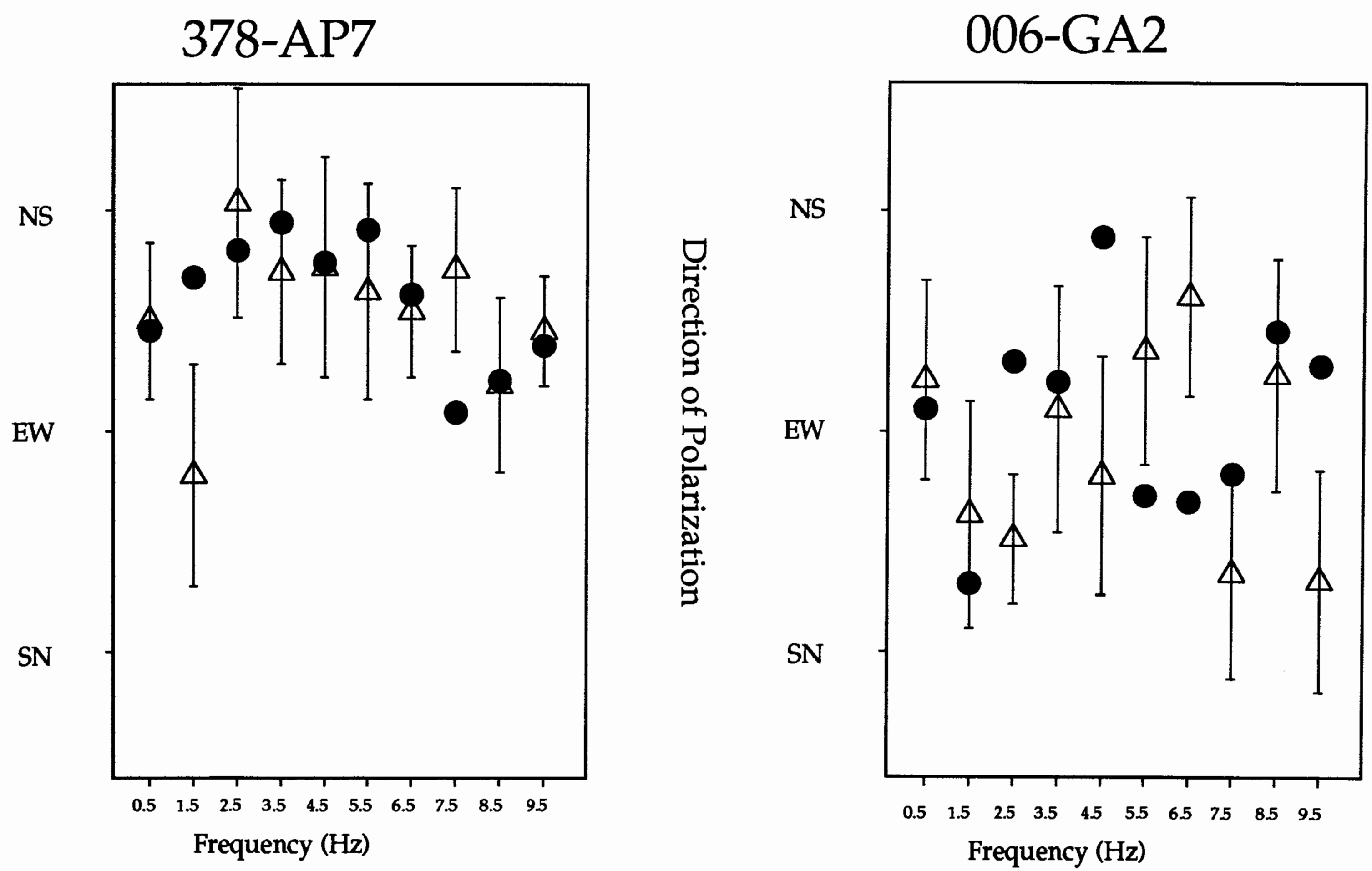

Figure 5. The open triangles show the mean direction of strongest shaking for 22 aftershocks in each frequency band. The error bars indicate one standard deviation. The solid circles show the direction of strongest shaking observed in the mainshock. a) Data from station 378/AP7. b) Data from station 006/GA2.

The coherence estimated in Figure 4 is examined in more detail in Figure 5. Here, the *mean* direction of motion for each frequency from the aftershocks is shown by an open triangle. The standard deviation is indicated by the error bar. The direction of motion in the mainshock is shown by the solid circles. The agreement at station 378/AP7 is striking (Figure 5a). For 8 out of 10 passbands, the mainshock direction of motion is within 30° of the aftershock mean motion. Note the very good agreement between the direction of shaking in the mainshock and the mean direction of shaking for the aftershocks, less than 5°, at the frequencies wheere the aftershock directions are most tightly clustered (0.5, 6.5, and 9.5 Hz). Station 006/AP7, on the other hand, shows little correlation between the (mostly poorly clustered) aftershock mean directions of strongest shaking and the mainshock directions of strongest shaking. This plot is also conservative. For example, excluding the 4 passbands where the mainshock polarization is least linear, fair to good agreement is seen in 5 of 6 passbands.

It appears that about 20 aftershock recordings were sufficient to provide fairly accurate "predictions" of the mainshock motion at one of the two stations presented. Rather surprisingly, it is the hard site (sandstone) rather than the alluvium that showed the stronger tendency for directional site resonance, emphasizing our poor understanding of the influence of the near-surface weathered layer.

NON-LINEAR SITE EFFECTS?

Non-linear effects are known to diminish the amplitude of very strong ground motion through conversion of seismic energy into heat in anelastic deformation. An understanding of non-linear damping is important, since most earthquake hazard research relies on the study of small earthquakes to predict the effects of big events. Non-linear effects have recently been proposed to occur in shaking as weak as 10% g by Chin and Aki (1991) and Darragh and Shakal (1991). The work of Chin and Aki (1991) requires assumptions about the seismic source, the attenuation of amplitude with distance, and the relation between horizontal vertical site response, while the work of Darragh and Shakal (1991) compares hard site-soft site pairs of stations, with the assumption that the hard rock site is free of strong site effects.

Another approach is to compare the amplitude of motions at a set of stations for an aftershock with that from the mainshock. In the ideal case of identical source location, identical mechanism, and no non-linear effects, the ratio of mainshock and aftershock motions should be constant across all stations for each frequency. So a plot of mainshock versus aftershock motion would produce a straight line whose slope is proportional to the ratio of the two earthquakes' source strengths.

We choose the 11 aftershocks ranging from magnitude 2.5 to 4.5 that are shown in Figure 6. The north-south and east-west components of each record are filtered into the passbands 1-2, 2-4, 4-8 and 8-12 Hz for each aftershock and the mainshock. We measure the larger of the peak amplitudes of the two components, and compare the mainshock with the aftershock motions for each passband in Figure 7.

These results are preliminary. The apparent saturation of mainshock motions suggests, however, that some non-linearity is present. In other words, in several cases the amplification observed for the mainshock is less than that seen in aftershocks, which could be due to non-linear damping of the mainshock motions. We must still correct for the differing moments and corner frequencies of the aftershocks. Several of the most discrepant points arise from the station in Capitola, making it the leading candidate for non-linear motions.

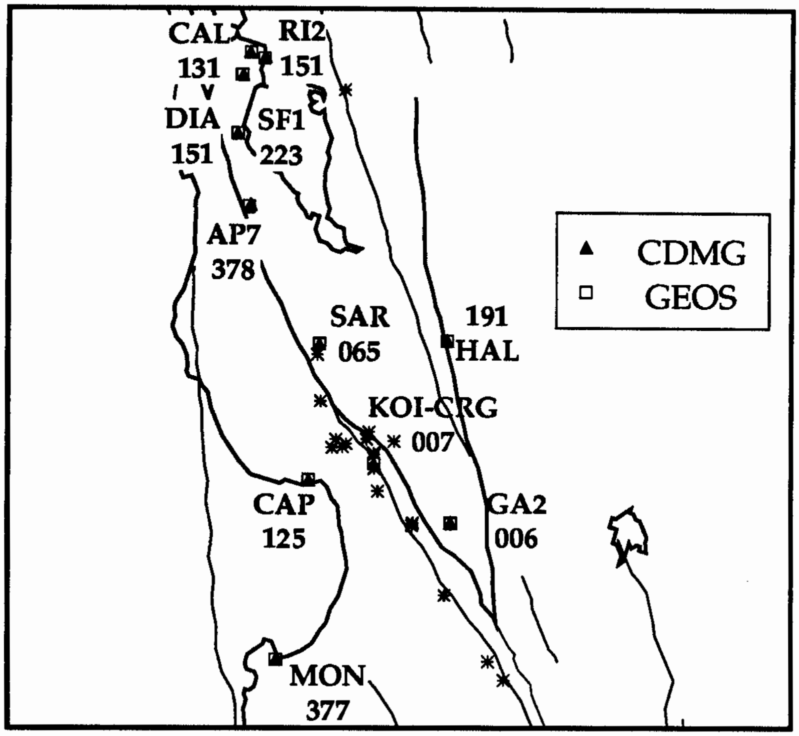

Figure 6. Map of the stations (triangles) that recorded the mainshock and the 11 aftershocks shown by circles.

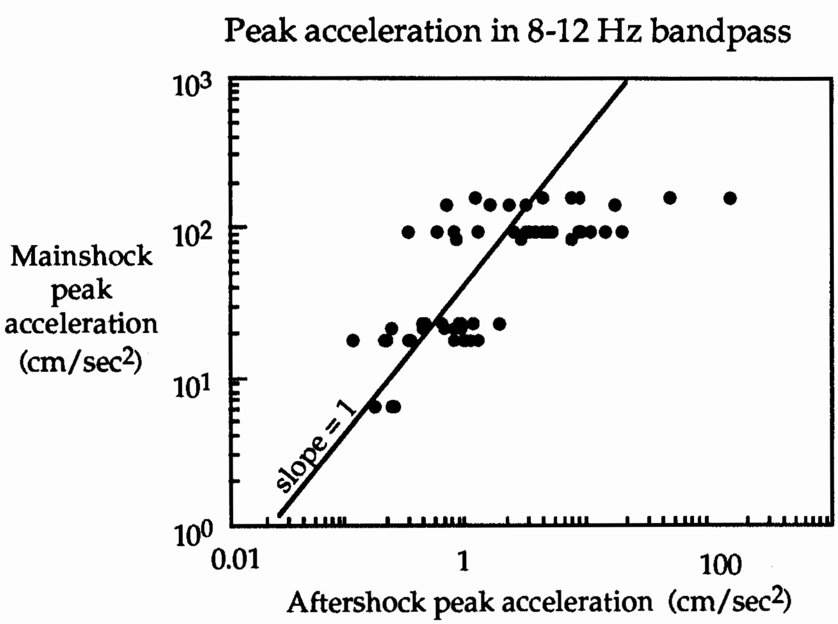

Figure 7. The amplitude of the peak motion in the mainshock plotted against the peak motion in each of the 11 aftershocks for the passband 8 to 12 Hz.

CONCLUSIONS AND UNANSWERED QUESTIONS

We have demonstrated that recordings of small earthquakes can provide useful estimates of directional resonance effects that occur in the mainshock. The evidence for non-linearity requires more thorough examination.

The remaining questions have advanced only incrementally since the meeting a year ago: Where are the geologic structures that strongly filter the high-frequency polarization characteristics? The low spatial coherence suggests shallow structure, borehole studies suggest shallow structure, and to the extent that common sense applies, the observation that the near surface is the least consolidated and most highly variable volume along the seismic ray path suggests that the structures lie near the surface. Candidates for these near surface structures include surface topography (Bard and Gariel, 1986, Kawase and Aki, 1989) and topography on the soil rock interface (Bard and Tucker, 1985). Candidates for wave interactions include focusing through seismic velocity gradients acting as lens (Rial, 1989, Langston and Lee, 1983), body-wave to surface-wave conversions at sharp, laterally heterogeneous velocity contrasts (Bard and Gariel, 1986, Vidale and Helmberger, 1988, Kawase and Aki, 1989), and energy that becomes trapped and reverberates between high contrast interfaces (Novaro et al., 1990).

The task remaining is the construction of simulations with methods like three-dimensional finite differences (Frankel *et al.*, 1990) that reproduce the complexity we observe in the seismic wavefield using realistic velocity models. This task relies on the equally difficult task of accurately estimating realistic three dimensional velocity models of the near surface.

REFERENCES

Abrahamson, N.A., J.F. Schneider, and J.C. Stepp, 1989. Spatial Coherency of strong ground motion for application to soil structure interaction, *Seism. Res. Lett.*, **60**, 3.

Aster, R., and P. Shearer, 1991. High-frequency seismic polarizations and site effects observed in boreholes in the San Jacinto fault zone, southern California. Part 1. Polarizations, *Bull. Seism. Soc. Am.* **81**,1057-1080.

Bard, P.-Y., and J.C. Gariel, 1986. The seismic response of two-dimensional sedimentary deposits with large vertical velocity gradients, *Bull. Seism. Soc. Am.*, **76**, 343-360.

Bard, P.-Y., and B.E. Tucker, 1985. Underground and ridge site effects: A comparison of observation and theory, *Bull. Seism. Soc. Am.*, **75**, 905-923.

Bonamassa, O., J.E. Vidale, H. Houston, and S.Y. Schwartz. Directional site resonances and the strong influence of near-surface geology on ground motion, *Geophys. Res. Lett.,* **18**, 901-904.

Bonamassa, O., J.E. Vidale, 1991. Directional site resonances observed from aftershocks of the 18 October 1989 Loma Prieta earthquake, *Bull. Seism. Soc. Am.*, **81**, 1945-57.

Borcherdt, R.D., 1970. Effects of local geology on ground motion near San Francisco Bay, *Bull. Seism. Soc. Am.*, **60**, 29-61.

Chin, B, and K. Aki, 1991. Simultaneous study of the source, path and site effects on strong ground motion during the 1989 Loma Prieta earthquake: A preliminary result on pervasive nonlinear site effects, *Bull, Seism. Soc. Am.*, **81**, 1859-1884.

Darragh, R.B., and A.F. Shakal, 1991. The site response of two rock and soil pairs to strong and weak ground motion, *Bull. Seism. Soc. Am.*, **81**, 1885-1899.

Dietel, C., B. Chouet, K. Aki, V. Ferrazzi, P. Roberts, and R.Y. Koyanagi, 1989. Data summary for dense GEOS array observations of seismic activity associated with magma transport at Kilauea Volcano, Hawaii, Open File Report, US Geological Society, 171 p.

Frankel, A., S. Hough, P. Friberg, R. Busby, 1991. Observations of Loma Prieta aftershocks from a dense array in Sunnyvale, California, *Bull. Seism. Soc. Am.*, **81**, 1900-1922.

Haukkson, E., T.-L. Teng, T.L. Henyey, 1987. Results from a 1500 m deep, three-level downhole seismometer array, *Bull. Seism. Soc. Am.*, **77**, 1883-1904.

Joyner, W.B., R.E. Warrick, T.E. Fumal, 1981. The effect of Quaternary alluvium on strong ground motion in the Coyote Lake, California, earthquake of 1979, *Bull. Seism. Soc. Am.*, **71**, 1333-1351.

Joyner, W.B., R.E. Warrick, and A.A. Oliver, III, 1976. Analysis of seismograms from a downhole array in sediments near San Francisco Bay, *Bull. Seism. Soc. Am.*, **66**, 937-958.

Kagami, H., S. Okada, K. Shiono, M. Oner, M. Dravinski, and A.K. Mal, 1986. Observation of 1-5 second microtremors and their application to earthquake engineering. Part III. A two-dimensional study of site effects in the San Fernando Valley, *Bull. Seism. Soc. Am.*, **76**, 1801-1812.

Kawase, H. and K. Aki, 1989. A study on the response of a soft basin for incident S, P, and Rayleigh waves with special reference to the long duration observed in Mexico City, *Bull. Seism. Soc. Am.*, **79**, 1361-1382.

Langston, C.A., and J. Lee, 1983. Effect of structure geometry on strong ground motions; the Duwamish river valley, Seattle, Washington, *Bull. Seism. Soc. Am.*, **73**, 1851-1863.

Malin, P.E., J.A. Waller, R.D. Borcherdt, E. Cranswick, E.G. Jensen, and N. Van Schaak, 1988. Vertical seismic profiling of Oroville microearthquakes: velocity spectra and particle motion as a function of depth, *Bull. Seism. Soc. Am.*, **78**, 401-420.

Menke, W., and A.Lerner-Lam, 1991. Observations of the transition from linear polarization to complex polarization in short-period compressive waves, *Bull. Seism. Soc. Am.*, **81**, 611-623.

Mueller, C., and G. Glassmoyer, 1990. Digital recordings of the aftershocks of the 17 October 1989 Loma Prieta, California, earthquake, US Geological Survey Open-file report 90-503, 147 p.

Novaro, O., T.H. Seligman, J.M. Alvarez-Tostado, J.L. Mateos, and J. Flores, 1990. Two-dimensional model for site effect studies of microtremors in the San Fernando Valley, *Bull. Seism. Soc. Am.*, **80**, 239-252.

Rial, J.A., 1989. Seismic wave resonance in 3-D sedimentary basins, *Geophys. J. Roy astr. Soc.*, **99**, 81-90.

Rogers, A.M., R.D. Borcherdt, P.A. Covington and D.M. Perkins, 1984. A comparative ground response study near Los Angeles using recordings of Nevada nuclear tests and the 1971 San Fernando earthquake, *Bull. Seism. Soc. Am.*, **74**, 1925-1949.

Vidale, J.E., 1986. Complex polarization analysis of particle motion, *Bull. Seism. Soc. Am.*, **76**, 1393-1406.

Vidale, J.E., and O. Bonamassa, 1992. Strong variations in strong motion recordings across San Francisco; the influence of near-surface geology, in press, *Loma Prieta Professional Paper*

Vidale, J.E., O. Bonamassa, and H. Houston, 1991. Directional Site Resonances Observed from the 1 October 1987 Whittier Narrows Earthquake and the 4 October Aftershock, *Earthquake Spectra.*, **7**, 107-126.

Vidale, J.E., and D.V. Helmberger, 1988. Elastic finite-difference modeling of the 1971 San Fernando, Ca. earthquake, *Bull. Seism. Soc. Am.*, **78**, 122-142.